Comparison of Thermal Infrared Emissivities Retrieved With the Two-Lid Box and the TES Methods With Laboratory Spectra

Maria Mira, Thomas J. Schmugge, *Fellow, IEEE*, Enric Valor, Vicente Caselles, and César Coll

***Abstract*—Knowledge of surface emissivity in the thermal infrared (TIR) region is critical for determining the land surface temperature (LST) from remote-sensing measurements. If emissivity is not well determined, it can cause a significant systematic error in obtaining the LST. The main aim of this paper is to compare different methods for measuring accurate land surface emissivity in the field, namely, the Box method and the Temperature and Emissivity Separation (TES) algorithm. Field emissivities were compared with soil spectra from laboratory measurements. Emissivities were measured for the bands of a multispectral radiometer CE312-2 with effective wavelengths at 8.4, 8.7, 9.1, 10.6, and 11.3 μm, similar to the Advanced Spaceborne Thermal Emission and Reflection Radiometer TIR bands, and a wide channel 8–13 μm. The measurements were made at two sites in New Mexico: the White Sands National Monument and an open shrub land in the Jornada Experimental Range. The measurements show that for both sites the emissivities derived with the Box method agree with those derived with the TES algorithm for the 10.6 and 11.3 μm bands. However, the emissivities for the shorter wavelength bands are higher when derived with the Box method than those with the TES algorithm, with differences ranging from 2% to 7%. The field emissivities agree within 2% with the laboratory spectrum for the 8–13-, 11.3-, and 10.6-μm bands. However, the field and laboratory measurements in general differ from 2.4% to 9% for the shorter wavelength bands, with the larger value most likely caused by variations in soil moisture.**

***Index Terms*—Algorithms, remote sensing, soil moisture, thermal infrared (TIR) emissivity.**

I. Introduction

EMISSIVITY (ε) is the physical property which defines the capability of a body to radiate and absorb energy from the environment. It is defined as the ratio between the real emission of an object and the emission of a black body at the object thermodynamic (or kinetic) temperature. If the emissivity is known, the land surface temperature (LST) can be accurately estimated from thermal infrared (TIR) radiance measurements. Mira *et al.* [1] observed that an emissivity variation of 0.06 causes an error of 2.2 K in the LST determination (at 11 μm and for an LST of about 300 K). Emissivity data are required as inputs of LST split-window algorithms [2], [3]. In addition, knowledge of the emissivity spectrum is useful to map geologic and land-cover materials based on differences in wavelength-dependent spectral features [4]–[7].

There are several studies that present different field methods to measure thermal emissivities [8]–[12]. The methods analyzed in this paper are the two-lid variant of the Box method [13] and the Temperature and Emissivity Separation (TES) algorithm [14].

The Box method, first proposed by Buettner and Kern [15] and Dana [16], allows the *in situ* determination of the TIR emissivities. It was improved through the two-lid variant of the Box method, described by Rubio *et al.* [13]. The method was developed to estimate the directional emissivity of homogeneous and elemental surfaces that may be part of a more complex structure such as composite pixels. According to Mira *et al.* [1], the two-lid variant of the Box method allows the determination of the emissivity with an average experimental error of $\pm 0.5\%$ at laboratory conditions.

The TES algorithm [14], [17] was developed to produce standard products of surface temperature and emissivity from Advanced Spaceborne Thermal Emission and Reflection radiometer (ASTER) data. However, it can also be applied to *in situ* measured at-ground TIR radiances when the downwelling sky irradiance is known. This method calculates a normalized temperature and an emissivity spectrum by means of the Normalized Emissivity Method (NEM) [18], [19]. Next, the Ratio algorithm [20] is applied to obtain the relative emissivities (the so-called β spectrum), which preserves the shape of the actual emissivity spectrum but not the amplitude. To obtain the amplitude and thus a better estimate of the LST, the maximum–minimum difference of β (MMD or spectral contrast) is calculated and used to predict the minimum emissivity ($\varepsilon_{\min}$) with the aid of an empirical relationship [21].

The objective of this paper is to analyze the accuracy of both field emissivity methods in the TIR domain. For this purpose, two different test sites were chosen, the first one characterized by relatively high spatial homogeneity in emissivity: White Sands and Jornada Experimental Range, New Mexico. A high-precision CIMEL Electronique CE 312-2 multispectral radiometer, whose channels are similar to the ASTER TIR

Manuscript received September 3, 2008; revised October 14, 2008 and October 23, 2008. Current version published March 27, 2009. This work was supported in part by the Spanish Ministry of Education and Science (*FPU* Research Grant of M. Mira) and Gerald Thomas endowment at New Mexico State University, by the Spanish Ministry of Education and Science projects (CGL2007-64666/CLI, CGL2004-06099-C03-01/CLI, CGL2006-27067-E/CLI, CGL2007-29819-E/CLI, CGL2007-28828-E/BOS), and by FEDER funds.

M. Mira, E. Valor, V. Caselles, and C. Coll are with the Department of Earth Physics and Thermodynamics, Faculty of Physics, University of Valencia, 46100 Burjassot, Spain (e-mail: Maria.Mira@uv.es; Enric.Valor@uv.es; Vicente.Caselles@uv.es; Cesar.Coll@uv.es).

T. J. Schmugge is with the Physical Science Laboratory, New Mexico State University, Las Cruces, NM 88003 USA (e-mail: tschmugge@psl.nmsu.edu).

Digital Object Identifier 10.1109/TGRS.2008.2008901

TABLE I
SAMPLE DESCRIPTION. CLAY SIZE IS CONSIDERED LESS THAN 0.002 mm, SILT SIZE RANGES FROM 0.002 TO 0.05 mm, AND SAND SIZE RANGES FROM 0.05 TO 2 mm

Sample	Characteristics	
Gypsum	Class	Entisol
	Subclass	Torripsamment
	Origin	Dona Ana Co., NM
	Organic carbon (%)	0.0
	Sand (%)	100.0
	Silt (%)	0.0
	Clay (%)	0.0
	Clay mineralogy	None
	Coarse mineralogy	Chemical analyzes indicate greater than 99% gypsum and a trace of quartz.
	Color	7.5Y8/1 light gray
Dark soil (site 3)	Class	Entisol
	Subclass	Torripsamment
	Origin	Jornada Experimental Range, Mesquite Site, NM
	Organic carbon (%)	< 0.5
	Sand (%)	81.0
	Silt (%)	7.5
	Clay (%)	11.5
	Color	10YR6/6 bright
Light soil (site 4)	Class	Entisol
	Subclass	Torripsamment
	Origin	Jornada Experimental Range, Mesquite Site, NM
	Organic carbon (%)	< 0.5
	Sand (%)	98.0
	Silt (%)	1.0
	Clay (%)	1.0
	Color	10YR6/4 dull yellow orange

bands, was used in the field in January and February 2008. Emissivities from the Box and TES methods were compared with high spectral resolution emissivity spectra of soil samples collected at White Sands and Jornada and measured with a Nicolet FTIR spectrophotometer [22]. A time series analysis of the emissivities for the Jornada site derived from ASTER data is presented by French *et al.* [23].

This paper proceeds as follows. The details of the experimental setup are shown in Section II, where the sites, the soil samples and the instrument are presented. Section III describes the methodology. The results and discussion of the experiment are analyzed in Section IV. Finally, Section V summarizes the main conclusions of this paper.

II. EXPERIMENTAL SETUP

A. Sites and Soil Samples

1) White Sands National Monument: The first site studied was the White Sands National Monument, located at about 25 km southwest of Alamogordo, Otero County, in southern New Mexico. The site is located in the mountain-ringed Tularosa Basin area and comprises the southern part of a 710-km^2 field of white sand dunes composed of gypsum crystals, at an elevation of about 1300 m.

The measurements were carried out on January 25, 2008. After exploring the area, two different locations within White Sands were chosen for this paper. Site 1 was on a dune crest with no vegetation and no footprints around, just wind-created ripples. In this case, this surface sand could be considered to be air-dried soil since it was easily blown by the wind. It was located at 32° 49′ 26″ N, 106° 16′ 23″ W. Site 2 was nearby and located within a flat interdune area with sparse vegetation and higher soil moisture than site 1. Its coordinates were 32° 49′ 27″ N, 106° 16′ 25″ W. For the year 2006, White Sands had 45 cm of rain, versus the usual 20 cm. In August 2006, it had 12.5 cm of rain, and the park was closed for almost a year due to flooding (David Bustos, personal communication). As a result, the gypsum in the lower interdune area had a slightly brown tint and a compact wet texture.

The gypsum soil texture is sand with particle sizes of about 330 μm. It is classified as Entisol Torripsamment according to soil taxonomy classification [24]. The sample description, provided by the ASTER Spectral Library (http://speclib.jpl.nasa.gov), is given in Table I.

2) Jornada Experimental Range: The second study site was placed in the Jornada Experimental Range (http://jornada-www.nmsu.edu), located in the northern Chihuahuan Desert, approximately 25 km northeast of Las Cruces, NM. It is located at 32.5° N, 106.8° W at an elevation of 1188 m and comprises 783 km^2. The Jornada Experimental Range is operated by the U.S. Department of Agriculture, Agricultural Research Service. This site belongs to the Long Term Ecological Research Network funded by the U.S. National Science Foundation.

The site is typical of desert grassland where the main vegetation components are grass and shrubs, such as black grama and honey mesquite, with a large fraction of exposed soil. The site has suffered significant degradation, with increases in shrub populations at the expense of the grasses.

The measurements at the Jornada were carried out on February 11, 2008. Two soils within the Mesquite area were chosen. The first one, located at 32° 39′ 2.9″ N, 106′ 52′ 12.4″ W, is a reddish brown compact soil. It will be referred to as the dark soil or site 3. The second soil, located at 32° 39′ 2.3″ N, 106° 52′ 12.7″ W, is a bright soil rich in

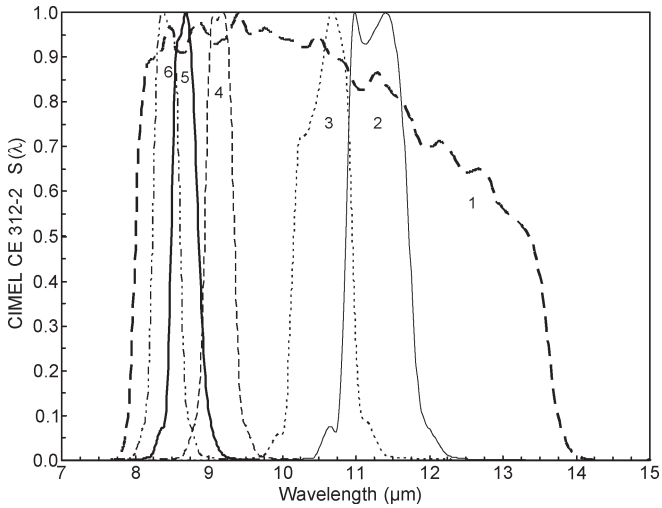

Fig. 1. Relative spectral response functions of the high-precision multichannel radiometer CIMEL Electronique CE 312-2.

quartz. It will be named as the light soil or site 4. The two sites are separated by about 10 m. This soil is a wind blown sand and covers about 20%–25% of the area generally accumulating near the base of shrubs. For more information about the type and amount of vegetation in the area, the reader is referred to French *et al.* [23].

The soil texture of these samples was determined according to the standard ISO 11277:1998 [25], based on sieving and mechanical sedimentation techniques. The results and descriptions are given in Table I.

B. Instrument: CIMEL Electronique CE 312-2[1]

Radiance measurements were carried out with the high-precision multichannel TIR radiometer CIMEL Electronique CE 312-2 [26]. It has six spectral channels: one broad and five narrow channels. Their relative spectral responses are shown in Fig. 1, and Table II shows the effective wavelength of each channel and their full-width at half-maximum. The radiometer has a field of view of 10° and a response time of 1 s. It was calibrated before the field measurements, and the calibration parameters were used for the data processing.

The similarity between the CE 312-2 bands and the ASTER TIR bands (see Table II) allows the application of the TES algorithm for recovering surface emissivities from the ground-based measurements.

III. Methodology

A. Box Method

The emissivities were determined through the two-lid variant of the Box method. Its methodology and rationale were analyzed in detail by Rubio *et al.* [27]. The Box method has the advantage of permitting the control of the environmental radiation by isolating the sample from the surroundings.

[1]Mention of a specific trade name or product is given for the benefit of the reader and implies no endorsement or preferential treatment by the company.

According to the Box method, the emissivity of the sample is obtained from a sequence of measurements of radiance in which a bottomless box with specular reflective walls is used. Two interchangeable lids with different spectral response are used as a top. One of them, whose emissivity is $\varepsilon_{\mathrm{h}} = 0.98$, is called the "hot lid" since its temperature is kept 15 °C–20 °C over that of the sample. The other lid is called the "cold lid" and has an emissivity $\varepsilon_{\mathrm{c}} = 0.03$. For an ideal box, $\varepsilon_{\mathrm{h}} = 1$ and $\varepsilon_{\mathrm{c}} = 0$. A thick insulating material covers the outer walls and lids of the box to insure the thermal homogeneity of the system. Moreover, the orientation of the box with respect to the Sun position was flipped during the measurements.

In the two-lid Box method, four measurements of radiance are performed with four different configurations of the box sample system. First, L^1 is measured by using the cold lid as top of the box and the sample as the bottom surface. Then, the system box-sample is equivalent to a black body at the sample temperature for the ideal box. Second, L^2 is measured by replacing the cold lid by the hot lid, which results in the radiance measured by the sensor corresponding to the radiance emitted by the sample plus the environmental irradiance (i.e., the hot lid irradiance that is reflected on the sample toward the sensor). Third, L^3 is measured by placing the box over a reflector similar to the cold lid. With this configuration and for an ideal box, it is equivalent to a black body at the hot lid temperature. Finally, L^4 is measured by using the cold lid as top and bottom of the box. In this way, the method gives the emissivity value of a sample as

$$\varepsilon = 1 - \frac{[L^2 - L^1](1 - \varepsilon_{\mathrm{c}})}{(L^3 - L^1) - [L^3 - L^2]P + (L^1 - L^4)Q} \quad (1)$$

where $P = 0.1460$ and $Q = 0.2921$ are factors which depend on the geometry of the box and the cold and hot lid emissivities. This fourth measurement is carried out to quantify the effect of a nonideal box (see [13]).

A series of five to ten emissivity measurements for each CE 312-2 channel was carried out in the field, and an average emissivity value from each series of measurements was calculated.

B. TES Algorithm

The TES algorithm was proposed by Gillespie *et al.* [14] to produce the Standard Products of surface temperature and emissivity from ASTER data. Here, a variant of the TES algorithm was applied to ground-based measurements from thermal multiband radiometers.

The TES algorithm is based on an empirical relationship between the range of emissivities for a set of TIR channels and their minimum value. It needs multispectral measurements, but does not require either multitemporal or multidirectional observations. For a multispectral TIR sensor with n-channels, there are $n + 1$ unknowns (n spectral emissivities plus one LST) but only n measurements, so additional information is required.

In TES, the ill-posed problem is addressed by combining three prior approaches to obtain an improved accuracy for the estimates of emissivity absolute values. The TES algorithm

TABLE II
EFFECTIVE WAVELENGTHS (λ_{eff}) AND FULL WIDTH AT HALF-MAXIMUM ($\Delta\lambda$) FOR THE BANDS OF THE RADIOMETER CE 312-2 AND THE ASTER TIR BANDS

CE 312-2 channel	λ_{eff} (μm)	$\Delta\lambda$ (μm)	ASTER TIR band	λ_{eff} (μm)	$\Delta\lambda$ (μm)
1	-	8.01 – 13.34	-	-	-
2	11.296	10.86 – 11.71	14	11.289	10.95 – 11.65
3	10.567	10.16 – 10.96	13	10.659	10.25 – 10.95
4	9.145	8.95 – 9.34	12	9.079	8.93 – 9.28
5	8.676	8.49 – 8.86	11	8.635	8.48 – 8.83
6	8.420	8.25 – 8.60	10	8.287	8.13 – 8.48

uses the MMD method proposed by Matsunaga [21], together with the NEM [18] to estimate surface radiometric temperature, from which emissivity ratios are derived using the Ratio algorithm [20]. The empirical relationship derived from laboratory spectral measurements of rocks, soils, vegetation, snow, and water [14], [17] is

$$\varepsilon_{\min} = 0.994 - 0.687\,\text{MMD}^{0.737}. \tag{2}$$

Using the CE 312-2, four measurements of the at-surface radiance, L_i^{surf} per channel, were made consecutively over each site at an observation angle close to nadir. Each channel measurement lasts 20 s, and therefore, the entire data take lasts 2 min (20 s × 6 channels). Five data sets of L_i^{surf} were measured over each site so that multiple emissivity spectra can be retrieved for comparisons. Close in time, a similar series of radiometric measurements of the sky at an observation angle of about 53° was made to estimate the downwelling atmospheric radiance. The sky irradiance, F_i^{sky} for each channel, is approximated as π times the downwelling sky radiance measured at the aforementioned angle [28]; this angle varies slightly with the atmospheric conditions and the spectral band. An average value of the sky measurements was used to characterize the downwelling sky irradiance. The TES algorithm was then applied, and finally, an average value of the retrieved spectral emissivities was calculated as well as its standard deviation. The use of a reference panel would have improved the measurement of the downwelling flux, but a reference panel was not available during the measurements in New Mexico. However, because the sky brightness is so low, and we had cloudless sky conditions and no tall trees or shrubs around, we expect that effect of errors in F_i^{sky} will be small.

To calculate the CE 312-2 wideband (8–13 μm) emissivity from TES measurements, the simplified expression of the radiative transfer equation was used

$$\varepsilon_i = \frac{L_i^{\text{surf}} - F_i^{\text{sky}}/\pi}{B_i(T) - F_i^{\text{sky}}/\pi} \tag{3}$$

where T is the retrieved LST and B_i is the black body radiance corresponding to the wideband channel i.

C. Laboratory High-Resolution Emissivity Spectra

High spectral resolution emissivity spectra of the soils, measured with a Nicolet FTIR spectrophotometer at the Jet Propulsion Laboratory (California Institute of Technology, Pasadena, CA), were analyzed. The spectrum of each soil from Jornada (for both site 3 and site 4) was available. A set of gypsum samples were collected at White Sands, in May 2008, and measured by Dr. Glynn Hulley. Spectra of eight samples of crests and three from interdune areas were considered as representatives of our site 1 and site 2 at White Sands. The samples from crests are dry, while samples from interdune areas are wet.

Each spectrum was convolved with the CE 312-2 spectral response functions, in order to obtain integrated values of emissivity comparable with our CIMEL measurements. The average value of the spectral emissivities for each site, and its standard deviation, were calculated. The error associated with the laboratory emissivities is $\delta(\varepsilon_{\text{lab}}) = \pm 0.002$ (see [22]). If a set of spectra were available, the calculated standard deviation of emissivity was considered when it was higher than ± 0.002. For additional details on the measurement technique, the reader is referred to the ASTER Spectral Library http://speclib.jpl.nasa.gov.

IV. RESULTS AND DISCUSSION

A. Comparison Between Emissivity Measurements

The emissivity values, along with their standard deviation, from the field measurements with the two methods over both sites of White Sands and Jornada are summarized in Tables III and IV, respectively. The measurements are also shown in Figs. 2 and 3, together with the laboratory spectra.

Using the standard deviation of the measurements as an indicator, there was a good agreement (better than 2%) between field and laboratory emissivities for the 8–13-, 11.3-, and 10.6-μm bands. However, the field and laboratory measurements in general differ from 2.4% to 9% for the shorter wavelength bands, i.e., 9.1, 8.7, and 8.4 μm. If the average value of the absolute difference between field and laboratory measurements is taken into account, both the Box and TES retrievals differ by about 2% from the laboratory spectra for gypsum, whereas for the Jornada soils the TES measurements agree significantly better (1.5%) than Box method (3%) with the laboratory measurements.

As shown in Tables III and IV, the average standard deviation of the emissivities derived with the Box method was 1.2%, while it was 0.15% for the TES algorithm. The spectral differences between both field methods are detailed in the last column of the tables. It is seen that there was generally a good agreement between methods for emissivities at 8–13, 11.3, and 10.6 μm. However, the Box retrievals are from 2% to 7% higher

TABLE III
FIELD AND LABORATORY EMISSIVITIES ε FOR THE WHITE SANDS SITES TOGETHER WITH THE STANDARD DEVIATION OF THE MEASUREMENTS $\delta(\varepsilon)$. THE EMISSIVITY DIFFERENCES BETWEEN FIELD METHODS, AND THE FIELD AND LABORATORY MEASUREMENTS ARE GIVEN AS WELL. $\Delta\varepsilon_\lambda$ IS THE SPECTRAL CONTRAST (MAXIMUM MINUS MINIMUM BAND EMISSIVITY), $\overline{\delta\varepsilon}$ IS THE AVERAGE STANDARD DEVIATION, AND $|\varepsilon_{\mathrm{field}} - \varepsilon_{\mathrm{lab}}|_{\mathrm{av}}$ IS THE AVERAGE OF ABSOLUTE DIFFERENCES

White Sands	Channel	$\varepsilon_{\mathrm{Box}}$	$\delta(\varepsilon_{\mathrm{Box}})$	$\varepsilon_{\mathrm{TES}}$	$\delta(\varepsilon_{\mathrm{TES}})$	$\varepsilon_{\mathrm{lab}}$	$\delta(\varepsilon_{\mathrm{lab}})$	$\varepsilon_{\mathrm{Box}}$-$\varepsilon_{\mathrm{lab}}$ (%)	$\varepsilon_{\mathrm{TES}}$-$\varepsilon_{\mathrm{lab}}$ (%)	$\varepsilon_{\mathrm{Box}}$-$\varepsilon_{\mathrm{TES}}$ (%)
Site 1	8 – 13 μm	0.931	0.010	0.9289	0.0012	0.940	0.003	-0.9	-1.1	0.2
	11.3 μm	0.962	0.010	0.9661	0.0005	0.977	0.002	-1.5	-1.1	-0.4
	10.6 μm	0.96	0.02	0.9601	0.0011	0.972	0.002	-1	-1.2	0.0
	9.1 μm	0.921	0.010	0.8983	0.0011	0.891	0.006	3	0.7	2.3
	8.7 μm	0.763	0.007	0.752	0.004	0.738	0.012	2.5	1.4	1.1
	8.4 μm	0.851	0.004	0.819	0.004	0.844	0.006	0.7	-2.5	3.2
$\Delta\varepsilon_\lambda$		0.202		0.214		0.239				
$\overline{\delta\varepsilon}$			0.010		0.002		0.005			
$\lvert\varepsilon_{\mathrm{field}}$-$\varepsilon_{\mathrm{lab}}\rvert_{\mathrm{av}}$ (%)								1.6	1.3	1.2
Site 2	8 – 13 μm	0.958	0.005	0.9375	0.0005	0.970	0.002	-1.2	-3.3	2.1
	11.3 μm	0.979	0.013	0.96059	0.00014	0.987	0.002	-0.8	-2.6	1.8
	10.6 μm	0.969	0.017	0.9537	0.0010	0.985	0.002	-1.6	-3.1	1.5
	9.1 μm	0.923	0.009	0.883	0.002	0.949	0.002	-2.6	-6.6	4.0
	8.7 μm	0.927	0.010	0.8825	0.0010	0.880	0.002	4.7	0.2	4.5
	8.4 μm	0.958	0.013	0.923	0.002	0.924	0.002	3.4	-0.1	3.5
$\Delta\varepsilon_\lambda$		0.056		0.078		0.107				
$\delta\varepsilon$			0.011		0.0011		0.002			
$\lvert\varepsilon_{\mathrm{field}}$-$\varepsilon_{\mathrm{lab}}\rvert_{\mathrm{av}}$ (%)								2.4	2.7	2.9

TABLE IV
FIELD AND LABORATORY EMISSIVITIES ε FOR THE JORNADA SITES TOGETHER WITH THE STANDARD DEVIATION OF THE MEASUREMENTS $\delta(\varepsilon)$. THE EMISSIVITY DIFFERENCES BETWEEN FIELD METHODS, AND THE FIELD AND LABORATORY MEASUREMENTS ARE GIVEN AS WELL. $\Delta\varepsilon_\lambda$ IS THE SPECTRAL CONTRAST (MAXIMUM MINUS MINIMUM BAND EMISSIVITY), $\overline{\delta\varepsilon}$ IS THE AVERAGE STANDARD DEVIATION, AND $|\varepsilon_{\mathrm{field}} - \varepsilon_{\mathrm{lab}}|_{\mathrm{av}}$ IS THE AVERAGE OF THE ABSOLUTE DIFFERENCES

Jornada	Channel	$\varepsilon_{\mathrm{Box}}$	$\delta(\varepsilon_{\mathrm{Box}})$	$\varepsilon_{\mathrm{TES}}$	$\delta(\varepsilon_{\mathrm{TES}})$	$\varepsilon_{\mathrm{lab}}\pm 0.002$	$\varepsilon_{\mathrm{Box}}$-$\varepsilon_{\mathrm{lab}}$ (%)	$\varepsilon_{\mathrm{TES}}$-$\varepsilon_{\mathrm{lab}}$ (%)	$\varepsilon_{\mathrm{Box}}$-$\varepsilon_{\mathrm{TES}}$ (%)
Site 3	8 – 13 μm	0.95	0.02	0.9168	0.0015	0.929	2.0	-1.2	3.0
	11.3 μm	0.992	0.005	0.95797	0.00008	0.966	2.6	-0.8	3.4
	10.6 μm	0.964	0.013	0.9458	0.0006	0.954	1.0	-0.8	1.8
	9.1 μm	0.875	0.003	0.8469	0.0013	0.872	0.3	-2.5	2.8
	8.7 μm	0.911	0.003	0.8689	0.0016	0.880	3.1	-1.1	4.2
	8.4 μm	0.915	0.009	0.8776	0.0008	0.868	4.7	1.0	3.7
$\Delta\varepsilon_\lambda$		0.117		0.111		0.098			
$\overline{\delta\varepsilon}$			0.009		0.0010				
$\lvert\varepsilon_{\mathrm{field}}$-$\varepsilon_{\mathrm{lab}}\rvert_{\mathrm{av}}$ (%)							2.3	1.2	3.2
Site 4	8 – 13 μm	0.868	0.007	0.8703	0.0019	0.864	0.4	0.6	-0.2
	11.3 μm	0.96	0.03	0.95283	0.00015	0.954	0.0	-0.1	1.0
	10.6 μm	0.94	0.02	0.9361	0.0016	0.931	1.0	0.5	0.0
	9.1 μm	0.759	0.017	0.7251	0.0011	0.692	6.7	3.3	3.4
	8.7 μm	0.80	0.03	0.734	0.003	0.704	9.0	3.0	7.0
	8.4 μm	0.765	0.008	0.722	0.003	0.698	6.7	2.4	4.3
$\Delta\varepsilon_\lambda$		0.198		0.230		0.262			
$\overline{\delta\varepsilon}$			0.018		0.0018				
$\lvert\varepsilon_{\mathrm{field}}$-$\varepsilon_{\mathrm{lab}}\rvert_{\mathrm{av}}$ (%)							4.0	1.7	2.7

than TES retrievals for the 9.1-, 8.7-, and 8.4-μm bands. The measurements show that the spectral contrast (maximum minus minimum band emissivity) $\Delta\varepsilon_\lambda$ for the TES algorithm was from 1.2% to 3.2% higher than for the Box method, except in site 3.

B. Soil Moisture Effect on Thermal Emissivities

As previously mentioned, the soil moisture for White Sands experimental test site 2 was higher than for site 1, which would cause an increase in the thermal emissivity [1], [10], [29]–[32]. Table V gives the differences between the field emissivities

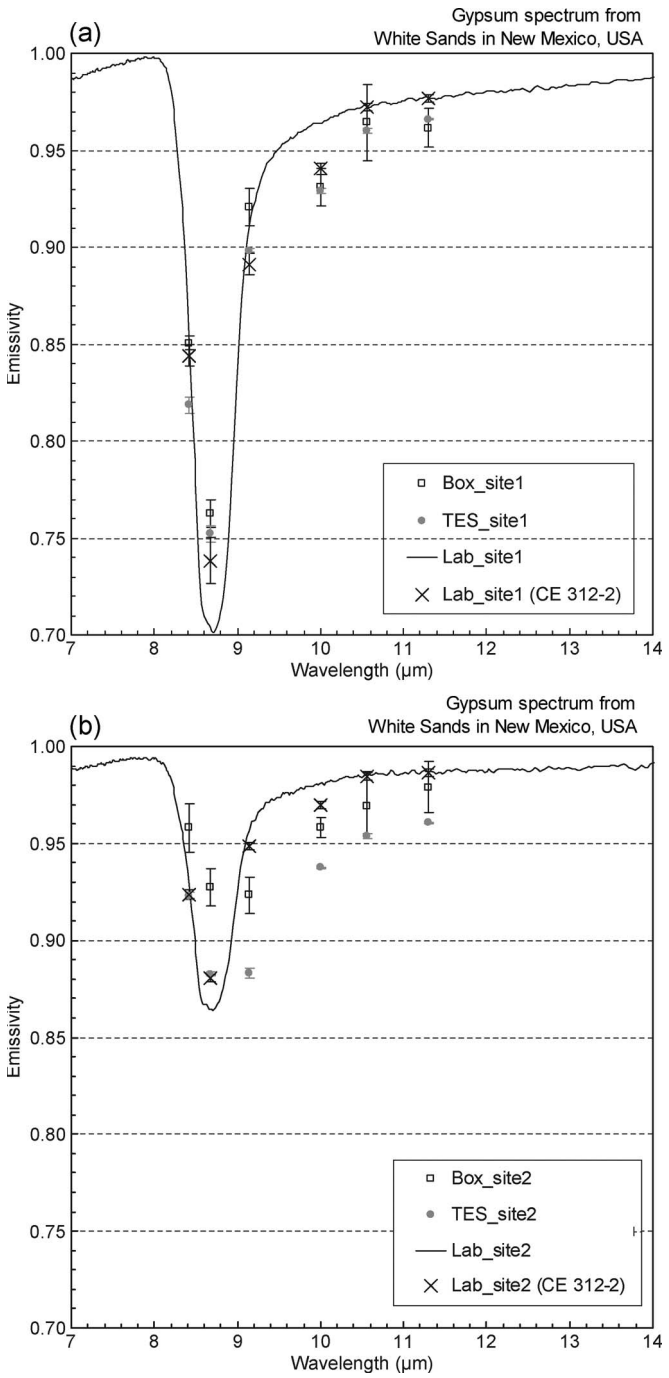

Fig. 2. Emissivity spectra of (a) air-dried gypsum from a dune crest (site 1) and (b) wet gypsum from a flat interdune area (site 2). Both soils are from the White Sands National Monument, New Mexico. Emissivities from the field measurements (Box method and TES algorithm) are represented by squares and dots, respectively. The solid lines show the average of the eight and three laboratory spectra considered as representatives of soils from site 1 and site 2, respectively. The crosses show the average value of the convolution of the set of eight or three spectra to the CE 312-2 bands, with the error bars showing the standard deviation of the measurements. The values at 10 μm are the wideband (8–13 μm) results.

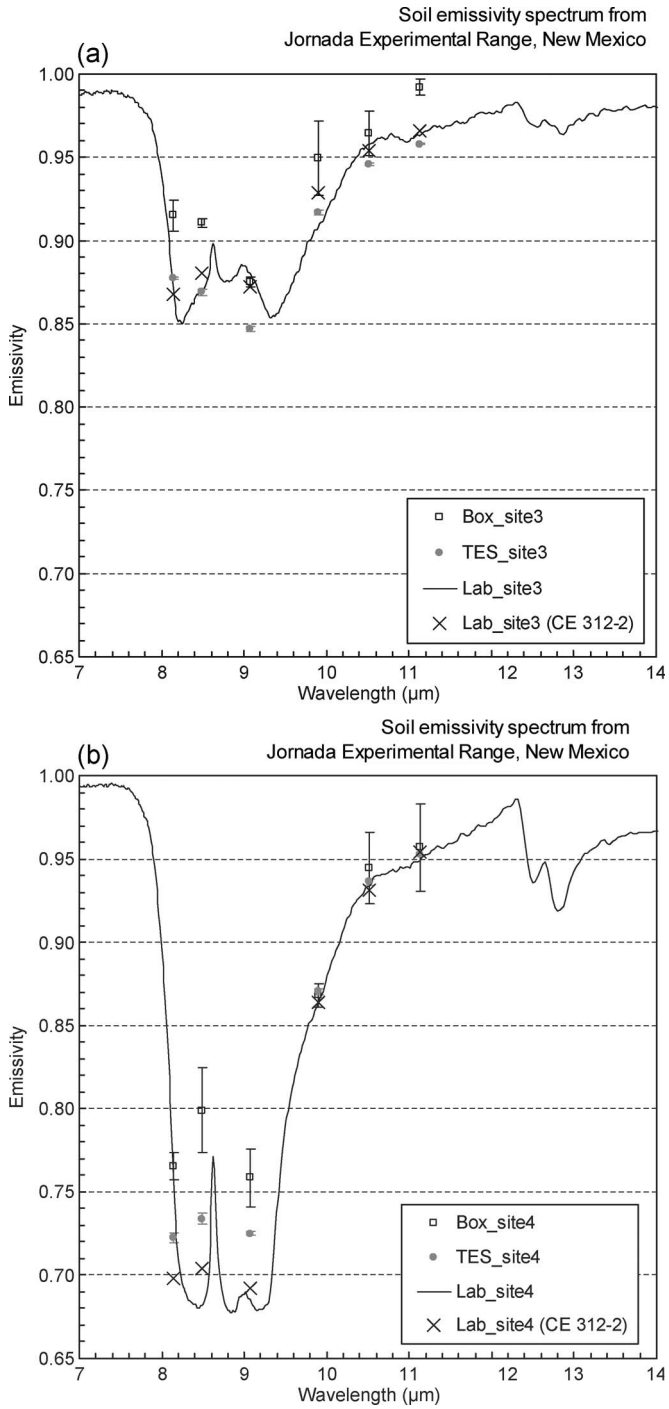

Fig. 3. Emissivity spectra of (a) dark soil (site 3) and (b) light soil (site 4) from Mesquite area in the Jornada Experimental Range, New Mexico. Emissivities from the field measurements (Box method and TES algorithm) are represented by squares and dots, respectively. The solid lines show the emissivity spectra from the laboratory measurements, with the crosses and the error bars showing the convolution to the CE 312-2 bands and the standard deviation of the measurements, respectively. The values at 10 μm are the wideband results.

measured at both sites. The ratio between the average emissivity for the short (8.4 μm, 8.7 μm, 9.1 μm) and long wavelength channels (10.6 μm, 11.3 μm) is presented as well.

After collecting and packing samples in the field, the volumetric soil moisture was measured in the laboratory with an SM200 soil moisture sensor several days later. The results showed a difference of about 20% in soil moisture between the two sites. According to Mira *et al.* [1], the 8.2–9.2-μm emissivity of sandy soils increases up to 16% when water content increased by 24%. Furthermore, the emissivity increase is not linear with soil moisture, being larger for low water contents. The measurements at White Sands agree with

TABLE V
SPECTRAL EMISSIVITY DIFFERENCE BETWEEN SITE 1 AND SITE 2 FROM WHITE SANDS, FOR BOTH FIELD METHODS AND LABORATORY MEASUREMENTS, AND EMISSIVITY RATIO OF AVERAGE CHANNELS (8.4 μm, 8.7 μm, 9.1 μm) : (10.6 μm, 11.3 μm), $\varepsilon_s/\varepsilon_l$. $\overline{\delta\varepsilon}$ IS THE AVERAGE STANDARD DEVIATION

White Sands						
Channel	$\varepsilon_{Box2}-\varepsilon_{Box1}$ (%)	$\delta(\varepsilon_{Box2}-\varepsilon_{Box1})$ (%)	$\varepsilon_{TES2}-\varepsilon_{TES1}$ (%)	$\delta(\varepsilon_{TES2}-\varepsilon_{TES1})$ (%)	$\varepsilon_{lab2}-\varepsilon_{lab1}$ (%)	$\delta(\varepsilon_{lab2}-\varepsilon_{lab1})$ (%)
8 – 13 μm	2.7	1.5	0.86	0.17	2.9	0.5
11.3 μm	2.0	2.0	-0.55	0.07	1.0	0.4
10.6 μm	1.0	4.0	-0.6	0.2	1.3	0.4
9.1 μm	0.3	1.9	-1.5	0.3	5.8	0.8
8.7 μm	16.5	1.7	13.0	0.5	14.2	1.4
8.4 μm	10.7	1.7	10.4	0.6	8.0	0.8
$\overline{\delta\varepsilon}$ (%)		2.0		0.3		0.7
	$(\varepsilon_s/\varepsilon_l)_{Box}$	$\delta(\varepsilon_s/\varepsilon_l)_{Box}$	$(\varepsilon_s/\varepsilon_l)_{TES}$	$\delta(\varepsilon_s/\varepsilon_l)_{TES}$	$(\varepsilon_s/\varepsilon_l)_{lab}$	$\delta(\varepsilon_s/\varepsilon_l)_{lab}$
Site 1	0.879	0.035	0.855	0.010	0.846	0.024
Site 2	0.961	0.044	0.936	0.006	0.931	0.007
Ratio increase between sites	0.082		0.081		0.085	

this result since the emissivities for the 8.7- and 8.4-μm bands increases from 10% to 17% between the two sites, an increase clearly larger than the experimental uncertainty (see Table V). The emissivity difference between sites is not significant for the 11.3- and 10.6-μm bands in agreement with previous studies [1], [31]. The emissivity increase due to soil moisture is further verified by the laboratory spectra, where emissivities for the 9.1-, 8.7-, and 8.4-μm bands increase from 6% to 14% between crest and interdune samples, with no significant changes being observed for the 11.3- and 10.6-μm bands.

The spectral contrast is reduced with soil moisture since water is very strongly absorbing in the region of the quartz reststrahlen bands (7.7 and 9.7 μm). According to this, Urai *et al.* [10] proposed the emissivity ratio of averaged ASTER TIR channels (10, 11, 12) : (13, 14) (i.e., similar to the emissivity ratio shown in Table V) as an indicator of the soil moisture content for sand with large amounts of quartz and feldspar. Laboratory measurements show an increase of 13% in this ratio when the moisture content of a sandy soil increases by 24% [1]. The emissivity measurements for gypsum soil at White Sands showed an increase of 8% in this ratio between the two sites for both field methods.

As previously mentioned, the soil measured at site 2 and the samples collected from the interdune areas could have different soil moisture content. Therefore, the difference in moisture content could explain the different emissivity values measured at site 2 in comparison with the laboratory spectrum. However, soil moisture does not explain the lower emissivity values from TES measurements in site 1 in comparison with laboratory measurements.

C. Sensitivity Analysis of the Methods

The sensitivity of the Box and the TES methods to the CE 312-2 radiometric error was analyzed. Two different cases were simulated: a gray body with emissivity $\varepsilon = 0.98$ like a vegetation surface, and a surface with a significant spectral contrast (spectral emissivities given in Table VI).

The basis of the simulation approach is the following: a Gaussian distribution, whose variance is equal to the accuracy of the radiometer and whose mean value is equal to zero, is considered for the radiometric error. A random value of this normal distribution is added to the temperatures measured by the CE 312-2. From these simulated measurements, the emissivities are calculated according both to the Box and the TES methods. Similar to the experimental technique, a set of simulated measurements is considered, and the average value of the emissivity and its standard deviation are finally calculated. The emissivity values obtained are compared with the original values used in the simulation.

The accuracies for each channel of the radiometer CE 312-2 when calibrated with a Landcal Blackbody Source (Type P80P) within the temperature range -10 °C to $+50$ °C are ± 0.30, ± 0.16, ± 0.18, ± 0.30, ± 0.17, and ± 0.30 K for channels 1 to 6, respectively. This calibration was carried out with an equivalent CE 312-2 radiometer at the University of Valencia.

For the simulations, the sample temperature was taken as the usual values for the different measurement sites of this paper, which were 4 °C, 12 °C, 24 °C, and 33 °C. In the case of the Box method, the "hot lid" temperatures were assumed to be 23 °C higher, and radiances for each ideal-Box configuration (i.e., L^1, L^2, and L^3) were calculated following [27, eqs. (4)–(6)]. For the TES method, the sky radiometric temperatures were taken as the typical clear-sky values measured in the four different sites, and the at-surface radiance was calculated from (3).

Table VI shows the results from both the Box and TES methods, for the simulation of a gray body and a high-contrast surface. It shows that the effect of the radiometric error of the instrument is slightly higher in the Box method ($\pm 1.2\%$) than in the TES method ($\pm 0.9\%$). Moreover, it is shown that there is not a significant systematic error, $|\varepsilon_{\rm ref} - \varepsilon_{\rm sim}|$, for the Box method, but it is about 0.9% and 2% for the TES method for a gray body and a high-contrast surface, respectively. This could explain partially the systematic differences obtained between the Box and TES measurements in field conditions (see Tables III and IV). Regarding the spectral contrast, $\Delta\varepsilon_\lambda$, it

TABLE VI
RESULTS OF THE EMISSIVITY SIMULATION (SUBSCRIPT "SIM") FROM THE SENSITIVITY ANALYSIS OF THE BOX AND TES METHODS, WHEN THEY ARE APPLIED IN THE FIELD WITH A CE 312-2 RADIOMETER. $\delta(\varepsilon)$ IS THE STANDARD DEVIATION AND THE SUBSCRIPT "REF" REFERS TO THE REFERENCE VALUE. $\Delta\varepsilon_\lambda$ IS THE SPECTRAL CONTRAST (MAXIMUM MINUS MINIMUM BAND EMISSIVITY), $\overline{\delta\varepsilon}$ IS THE AVERAGE STANDARD DEVIATION, AND $|\varepsilon_{\rm ref} - \varepsilon_{\rm sim}|_{\rm av}$ IS THE AVERAGE OF THE ABSOLUTE DIFFERENCES

			Box			TES		
	Channel	$\varepsilon_{\rm ref}$	$\varepsilon_{\rm sim}$	$\delta(\varepsilon)_{\rm sim}$	$\varepsilon_{\rm ref}-\varepsilon_{\rm sim}$ (%)	$\varepsilon_{\rm sim}$	$\delta(\varepsilon)_{\rm sim}$	$\varepsilon_{\rm ref}-\varepsilon_{\rm sim}$ (%)
Gray body	8 – 13 μm	0.980	0.979	0.015	0.1	0.972	0.018	0.8
	11.3 μm	0.980	0.980	0.008	0.0	0.972	0.006	0.8
	10.6 μm	0.980	0.980	0.010	0.0	0.973	0.006	0.7
	9.1 μm	0.980	0.980	0.015	0.0	0.970	0.007	1.0
	8.7 μm	0.980	0.980	0.008	0.0	0.970	0.008	1.0
	8.4 μm	0.980	0.979	0.016	0.1	0.969	0.011	1.1
	$\Delta\varepsilon_\lambda$	0.000	0.001			0.004		
	$\overline{\delta\varepsilon}$			0.012			0.009	
	$\lvert\varepsilon_{\rm ref}-\varepsilon_{\rm sim}\rvert_{\rm av}$ (%)				0.0			0.9
High-contrast surface	8 – 13 μm	0.945	0.947	0.014	-0.2	0.960	0.017	-1.5
	11.3 μm	0.978	0.978	0.008	0.0	0.961	0.002	1.7
	10.6 μm	0.974	0.974	0.009	0.0	0.956	0.005	1.8
	9.1 μm	0.872	0.871	0.013	0.1	0.855	0.008	1.7
	8.7 μm	0.835	0.835	0.007	0.0	0.815	0.004	2.0
	8.4 μm	0.965	0.964	0.015	0.1	0.942	0.010	2.4
	$\Delta\varepsilon_\lambda$	0.143	0.143			0.146		
	$\overline{\delta\varepsilon}$			0.011			0.008	
	$\lvert\varepsilon_{\rm ref}-\varepsilon_{\rm sim}\rvert_{\rm av}$ (%)				0.1			1.9

TABLE VII
DIFFERENCES BETWEEN THE INTERPOLATED (SUBSCRIPT t_s) AND MEASURED TEMPERATURES FOR THE CE 312-2 CHANNELS

	White Sands		Jornada	
Channel	$\lvert T^{\rm surf}_{ts}-T^{\rm surf}\rvert$ (K)	$\lvert T^{\rm sky}_{ts}-T^{\rm sky}\rvert$ (K)	$\lvert T^{\rm surf}_{ts}-T^{\rm surf}\rvert$ (K)	$\lvert T^{\rm sky}_{ts}-T^{\rm sky}\rvert$ (K)
8 – 13 μm	0.018	0.06	0.10	0.03
11.3 μm	0.019	0.12	0.11	0.08
10.6 μm	0.007	0.02	0.10	0.3
9.1 μm	0.09	0.11	0.07	0.16
8.7 μm	0.08	0.04	0.06	0.11
8.4 μm	0.10	0.14	0.07	0.07

was slightly better preserved by the Box method (within 0.1%) than the TES algorithm (within 0.4%).

D. Nonsimultaneity of the TES Measurements

The simultaneous measurement of the spectral radiances for the TES method is not possible with the CE 312-2 radiometer. As noted in Section III-B, the CE 312-2 takes 2 min to make the entire data set of four measurements per each of the six spectral channels. The influence of the nonsimultaneity of the measurements on the emissivity values retrieved by the TES method is analyzed in this section.

Since several data sets were measured continuously at a site, it is possible to assess the temporal variation of the measured temperatures for a given channel. The time at the center of each data set was taken ($t_s = 1$ min). For this t_s, we obtained the corresponding temperature for each channel by linear interpolation between two consecutive data sets.

Table VII shows that the difference between the measured and interpolated radiometric temperatures is less or of the same order than the accuracy of the CE 312-2 channels. The TES emissivities retrieved from the interpolated and the measured temperatures are the same for the 11.3- and 10.6-μm channels, and differences less than 0.2% are obtained for the 9.1-, 8.7-, 8.4-, and 8–13-μm channels, which is less than the standard deviation of the TES measurements. In conclusion, the nonsimultaneity of the TES measurements did not affect the emissivity retrievals in our experiments. This may not be true for windy or cloudy days when large variations in temperature can occur in short times.

The simultaneous measurement of surface and sky temperatures might be possible with the use of a pair of radiometers but a second one was not available. Possible changes in the downwelling sky radiance should not be skipped over. However, variations in sky temperature are lower than those in LST, and also their influence into TES retrievals is reduced because of the low reflectivity for soils. As a result, we can conclude as well that the nonsimultaneity of surface and sky temperature measurements with the CE 312-2 did not significantly affect the emissivity retrievals in our experiments.

V. Summary and Conclusions

In this paper, two methods for measuring TIR emissivities in the field were studied: the two-lid variant of the Box method and the TES algorithm. An analysis of the comparison between their retrievals were performed. Two areas were used to conduct the study. The first area was the White Sands National Monument and the second the Jornada Experimental Range.

A high-precision multichannel TIR radiometer CIMEL Electronique CE 312-2 was used for the radiance measurements, and because its bands were designed to be similar to those of ASTER, it was possible the use of the same TES algorithm. Additionally, high-resolution emissivity spectra of each kind of soil measured at the laboratory were compared with the field measurements.

When comparing field and laboratory emissivity measurements, there is an agreement better than 3% for the longer wavelength bands at 10.6-, 11.3-, and 8–13-μm band. However, the Box method retrieves higher emissivity values than the TES algorithm on the spectral bands at the 8- to 9-μm range, where the studied soils have a strong emissivity minimum due to the quartz reststrahlen band of quartz. The differences ranged from 2% to 7%, which correspond to an error in LST from 0.7 to 2.6 K. Furthermore, field emissivities differ from laboratory spectra from 2.4% to 9% in these bands, which correspond to an error in LST from 0.9 to 3.3 K and is most likely caused by variations in soil moisture.

The study showed the influence of soil moisture on thermal emissivities as well. An emissivity increase up to 17% in the 8- to 9-μm range and an increase of 8% in emissivity ratio of average channels (8.4 μm, 8.7 μm, 9.1 μm) : (10.6 μm, 11.3 μm) were measured for two gypsum samples with different water content.

The sensitivity analysis performed for the Box and TES methods showed that the uncertainty introduced by the radiometric error of the instrument is about $\pm 1.2\%$ and $\pm 0.9\%$, respectively. Moreover, no systematic error was observed for the Box method, but it was 0.9% and 2% for the TES method when a gray body and a nongray body were considered, respectively. This could explain the systematic differences observed between the measurements of both field methods.

The results obtained for the Box and the TES methods in this experiment show that the agreement with laboratory spectra is better for TES method in some sites. However, there are more aspects to take into account. We note that the measurement time for the TES method (about 20 min) is much shorter than that for the Box method (about 1 h). Furthermore, neither box nor additional power is needed to carry out the TES measurements, which makes this method more practical than the Box method. Besides, the sensitivity analysis showed that there is a systematic error (up to 2%) for the TES emissivities, which is larger for larger MMD. Since the emissivity at the longer TIR wavelengths shows less variability, the Box emissivity for the 11.3-μm band could be used as a reference to correct the TES curve shape. Approximately the same emissivities are obtained from (3) when considering the LST obtained from the reference emissivity (Box emissivity at the 11.3-μm band). However, in both cases, the agreement of TES with the Box emissivities of our experiments is not as good as desirable: the differences between their retrievals are still up to 4%, which correspond to an error in LST up to 1.5 K.

Acknowledgment

The authors would like to thank Dr. G. Hulley, from the Jet Propulsion Laboratory (Pasadena, CA), for providing us with laboratory spectra of gypsum samples from White Sands. The authors would also like to thank the two reviewers for their constructive remarks and comments.

References

[1] M. Mira, E. Valor, R. Boluda, V. Caselles, and C. Coll, "Influence of soil water content on the thermal infrared emissivity of bare soils: Implication for land surface temperature determination," *J. Geophys. Res.*, vol. 112, no. F4, p. F04 003, 2007. DOI: 10.1029/2007JF000749.

[2] Y. Yu, J. P. Privette, and A. C. Pinheiro, "Evaluation of split-window land surface temperature algorithms for generating climate data records," *IEEE Trans. Geosci. Remote Sens.*, vol. 46, no. 1, pp. 179–192, Jan. 2008.

[3] J. M. Galve, C. Coll, V. Caselles, and E. Valor, "An Atmospheric Radiosounding database for generating land surface temperature algorithms," *IEEE Trans. Geosci. Remote Sens.*, vol. 46, no. 5, pp. 1547–1557, May 2008.

[4] L. C. Rowan, J. C. Mar, and C. J. Simpson, "Lithologic mapping of the Mordor, NT, Australia ultramafic complex by using the Advanced Spaceborne Thermal Emission and Reflection Radiometer (ASTER)," *Remote Sens. Environ.*, vol. 99, no. 1/2, pp. 105–126, Nov. 2005.

[5] R. G. Vaughan, S. J. Hook, W. M. Calvin, and J. V. Taranik, "Surface mineral mapping at Steamboat Springs, Nevada, USA, with multi-wavelength thermal infrared images," *Remote Sens. Environ.*, vol. 99, no. 1/2, pp. 140–158, Nov. 2005.

[6] I. F. Trigo, L. F. Peres, C. C. DaCamara, and S. C. Freitas, "Thermal land surface emissivity retrieved from SEVIRI/Meteosat," *IEEE Trans. Geosci. Remote Sens.*, vol. 46, no. 2, pp. 307–314, Feb. 2008.

[7] K. Ogawa, T. Schmugge, and S. Rokugawa, "Estimating broadband emissivity of arid regions and its seasonal variations using thermal infrared remote sensing," *IEEE Trans. Geosci. Remote Sens.*, vol. 46, no. 2, pp. 334–343, Feb. 2008.

[8] P. R. Christensen and S. T. Harrison, "Thermal infrared-emission spectroscopy of natural surfaces—Application to desert varnish coatings on rocks," *J. Geophys. Res.*, vol. 98, no. B11, pp. 19 819–19 834, 1993.

[9] J. W. Salisbury, A. Wald, and D. M. D'Aria, "Thermal-infrared remote sensing and Kirchhoff's law 1. Laboratory measurements," *J. Geophys. Res.*, vol. 99, no. B6, pp. 11 897–11 911, 1994.

[10] M. Urai, T. Matsunaga, and T. Ishii, "Relationship between soil moisture content and thermal infrared emissivity of the sand sampled in Muus Desert, China," *J. Remote Sens. Soc. Jpn.*, vol. 17, no. 4, pp. 322–331, 1997.

[11] Y. Ninomiya, T. Matsunaga, Y. Yamaguchi, K. Ogawa, S. Rokugawa, K. Uchida, H. Muraoka, and M. Kaku, "A comparison of thermal infrared emissivity spectra measured *in situ*, in the laboratory, and derived from thermal infrared multispectral scanner (TIMS) data in Cuprite, Nevada, U.S.A.," *Int. J. Remote Sens.*, vol. 18, no. 7, pp. 1571–1581, May 1997.

[12] Z. Wan, "New refinements and validation of the MODIS land-surface temperature/emissivity products," *Remote Sens. Environ.*, vol. 112, no. 1, pp. 59–74, Jan. 2008.

[13] E. Rubio, V. Caselles, C. Coll, E. Valor, and F. Sospedra, "Thermal-infrared emissivities of natural surfaces: Improvements on the experimental set-up and new measurements," *Int. J. Remote Sens.*, vol. 24, no. 24, pp. 5379–5390, Dec. 2003.

[14] A. Gillespie, S. Rokugawa, T. Matsunaga, J. S. Cothern, S. Hook, and A. B. Kahle, "A temperature and emissivity separation algorithm for Advanced Spaceborne Thermal Emission and Reflection Radiometer (ASTER) images," *IEEE Trans. Geosci. Remote Sens.*, vol. 36, no. 4, pp. 1113–1126, Jul. 1998.

[15] K. J. K. Buettner and C. D. Kern, "The determination of infrared emissivities of terrestrial surfaces," *J. Geophys. Res.*, vol. 70, pp. 1329–1337, 1965.

[16] R. W. Dana, "Measurement of 8–14 micron emissivity of igneous rocks and mineral surfaces," Goddard Space Flight Center, Greenbelt, MD, NASA Sci. Rep. NSG-632, 1969.

[17] T. J. Schmugge, S. J. Hook, and C. Coll, "Recovering surface temperature and emissivity from thermal infrared multispectral data," *Remote Sens. Environ.*, vol. 65, no. 2, pp. 121–131, Aug. 1998.
[18] A. R. Gillespie, "Lithologic mapping of silicate rocks using TIMS," in *Proc. TIMS Data Users' Workshop*, Pasadena, CA, 1986, pp. 29–44. Jet Propulsion Lab. Pub. 86-38.
[19] V. J. Realmuto, "Separating the effects of temperature and emissivity: Emissivity spectrum normalization," in *Proc. 2nd TIMS Workshop*, Pasadena, CA, 1990, pp. 23–27. Jet Propulsion Lab. Pub. 90–55.
[20] K. Watson, "Spectral ratio method for measuring emissivity," *Remote Sens. Environ.*, vol. 42, no. 2, pp. 113–116, Nov. 1992.
[21] T. Matsunaga, "A temperature-emissivity separation method using an empirical relationship between the mean, the maximum and the minimum of the thermal infrared emissivity spectrum," *J. Remote Sens. Soc. Jpn.*, vol. 14, no. 2, pp. 230–241, 1994.
[22] A. R. Korb, J. W. Salisbury, and D. M. D'Aria, "Thermal-infrared remote sensing and Kirchhoff's law. 2. Field measurements," *J. Geophys. Res.*, vol. 104, no. B7, pp. 15 339–15 350, 1999.
[23] A. N. French, T. J. Schmugge, J. C. Richie, A. Hsu, F. Jacob, and K. Ogawa, "Detecting land cover change at the Jornada Experimental Range, New Mexico with ASTER emissivities," *Remote Sens. Environ.*, vol. 112, no. 4, pp. 1730–1748, Apr. 2008.
[24] "Soil taxonomy. A basic system of soil classification for making and interpreting soil surveys," *Agriculture Handbook 436*, Soil Survey Staff, U.S. Dept. Agric., Washington, DC, 1999.
[25] International Organization for Standardization, "Soil quality. Determination of particle size distribution in mineral soil material. Method by sieving and sedimentation," Geneva, Switzerland, Rep. ISO 11277:1998/TC190, 2002.
[26] G. Brogniez, C. Pietras, M. Legrand, P. Dubuisson, and M. Haeffelin, "A high-accuracy multiwavelength radiometer for *in situ* measurements in the thermal infrared. Part II: Behavior in field experiments," *J. Atmos. Ocean Technol.*, vol. 20, no. 7, pp. 1023–1033, Jul. 2003.
[27] E. Rubio, V. Caselles, and C. Badenas, "Emissivity measurements of several soils and vegetation types in the 8–14 μm wave band: Analysis of two field methods," *Remote Sens. Environ.*, vol. 59, no. 3, pp. 490–521, Mar. 1997.
[28] K. Y. Kondratyev, *Radiation in the Atmosphere*. New York: Academic, 1969.
[29] J. M. Chen, B. J. Yang, and R. H. Zhang, "Soil thermal emissivity as affected by its water content and surface treatment," *Soil Sci.*, vol. 148, no. 6, pp. 433–435, 1989.
[30] J. W. Salisbury and D. M. D'Aria, "Infrared (8–14 μm) remote sensing of soil particle size," *Remote Sens. Environ.*, vol. 42, no. 2, pp. 157–165, Nov. 1992.
[31] Q. Xiao, Q. H. Liu, X. W. Li, L. F. Chen, Q. Liu, and X. Z. Xin, "A field measurement method of spectral emissivity and research on the feature of soil thermal infrared emissivity," *J. Infrared Millim. Waves*, vol. 22, no. 5, pp. 373–378, 2003.
[32] K. Ogawa, T. J. Schmugge, and S. Rokugawa, "Observations of soil moisture dependence of thermal infrared emissivity on soil moisture," *Geophys. Res. Abstr.*, vol. 8, p. 04 996, 2006.

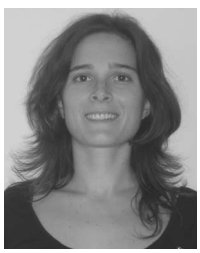

Maria Mira was born in Ontinyent, Spain, in 1982. She received the B.Sc. degree (first-class honors) in physics and the M.Sc. degree in environmental physics and thermodynamics from the University of Valencia, Burjassot, Spain, in 2005 and 2007, respectively, where she is currently working toward the Ph.D. degree in physics from the University of Valencia, Spain.

From December 2007 to March 2008, she was a Visiting Student with New Mexico State University, Las Cruces. Her research interest focuses on the physical processes of thermal infrared remote sensing, including the retrieval of surface emissivity from thermal infrared remote sensed data supplied by the Moderate Resolution Imaging Spectroradiometer and the Advanced Spaceborne Thermal Emission and Reflection Radiometer sensors, as well as by field radiometers.

Thomas J. Schmugge (M'83–SM'91–F'01) received the B.S. degree in physics from the Illinois Institute of Technology, Chicago, in 1959 and the Ph.D. degree in physics from the University of California, Berkeley, in 1965.

From 1964 to 1970, he was an Assistant Professor of physics with Trinity College, Hartford, CT. For 15 years (1970–1986), he was with the Hydrological Sciences Branch, Goddard Space Flight Center, National Aeronautics and Space Administration, Greenbelt, MD. In January 2004, he retired from the Hydrology and Remote Sensing Laboratory, Agricultural Research Service, U.S. Department of Agriculture, Beltsville, MD, where he worked on the application of remote-sensing techniques to the study of land surface hydrologic processes. From 2005 to 2008, he was the Gerald Thomas Professor of Water Resources with New Mexico State University (NMSU), Las Cruces. Currently, he is with the Physical Science Laboratory, NMSU. He has published more than 250 papers on the application of remote sensing to hydrologic problems, more than half of which appeared in peer-reviewed journals. His research interests include the use of microwave and thermal infrared remote-sensing techniques to observe such parameters as surface temperature and emissivity, soil moisture, and evapotranspiration. He is an Adjunct Member of the Joint U.S./Japan Advanced Spaceborne Thermal Emission and Reflection Radiometer Science Team.

Dr. Schmugge is a Fellow of the American Geophysical Union (AGU). He received the Robert E. Horton Medal in Hydrology from the AGU in 2006. He is an Associate Editor for the IEEE TRANSACTIONS ON GEOSCIENCE AND REMOTE SENSING.

Enric Valor received the B.Sc., M.Sc., and Ph.D. degrees in physics from the University of Valencia, Burjassot, Spain, in 1992, 1994, and 1997, respectively.

He is currently an Associate Professor of earth physics with the Department of Earth Physics and Thermodynamics, Faculty of Physics, University of Valencia. He has published 35 papers in international journals and 45 conference papers. His research interest focuses on the physical processes of thermal infrared remote sensing, emissivity measurement and characterization, atmospheric and emissivity corrections, and temperature emissivity separation algorithms.

Vicente Caselles received the B.Sc., M.Sc., and Ph.D. degrees in physics from the University of Valencia, Burjassot, Spain, in 1979, 1980, and 1983, respectively.

He is currently a Professor of applied physics and the Head of the Thermal Remote Sensing Group, Department of Earth Physics and Thermodynamics, Faculty of Physics, University of Valencia. He has expertise of 30 years in the physical processes involved in the temperature measurement using remote-sensing techniques, which has been documented through 10 books, 20 doctoral theses, 100 papers in international journals, 60 conference papers, and 30 reports. He was collaborating with the European Space Agency as a member of the Advisory Group for the Land-Surface Processes and Interactions Mission. He was the Chairman of the Spanish Remote Sensing Society, and he is currently the Manager of the Spanish Atmosphere and Climate Program.

César Coll received the B.Sc., M.Sc., and Ph.D. degrees in physics from the University of Valencia, Burjassot, Spain, in 1989, 1992, and 1994, respectively.

He is currently an Associate Professor of earth physics with the Department of Earth Physics and Thermodynamics, Faculty of Physics, University of Valencia. He has published 40 papers in international journals and 50 conference papers. His research interest focuses on the physical processes of thermal infrared (TIR) remote sensing, atmospheric and emissivity corrections, temperature emissivity separation, and ground validation of Advanced Along Track Scanning Radiometer, Moderate Resolution Imaging Spectroradiometer, and Advance Spaceborne Thermal Emission and Reflection Radiometer TIR products.